Sharpening up the charged Higgs boson signature using τ polarization at the CERN LHC

Sreerup Raychaudhuri and D. P. Roy*
Theoretical Physics Group, Tata Institute of Fundamental Research, Homi Bhabha Road, Bombay 400 005, India
(Received 17 October 1995)

The opposite states of the τ polarization resulting from the charged Higgs boson and the W boson decays can be exploited to enhance the $H^{\pm}$ signal in the inclusive one-prong hadronic decay channel of τ. We suggest practical methods of sharpening up the $H^{\pm}$ signature in the top quark decay at the CERN LHC using this idea. As a result one can carry on the charged Higgs boson search to within ~20 GeV of the parent top quark mass over the full parameter space of the MSSM. [S0556-2821(96)04409-8]

PACS number(s): 14.80.Cp, 13.85.Qk, 13.88.+e, 14.60.Fg

I. INTRODUCTION

A direct top quark signal has been recently observed at the Fermilab Tevatron collider [1] with

$$m_t \simeq 175 \ \text{GeV}, \tag{1}$$

which also agrees with the indirect estimate of top quark mass from the CERN e^+e^- collider LEP [2]. One expects a couple of dozens of clearly identifiable top quark events at the end of the current Tevatron run, which would go up to a few hundred following the upgradation of its luminosity via the main injector. The corresponding number of identifiable top quark events at the CERN Large Hadron Collider (LHC) is expected to be of the order of 10^6 per year, i.e., similar to the rate of Z boson events at LEP. Thus, the LHC is expected to serve as a top quark factory, which will enable us to make a detailed study of its decay and, in particular, to search for new particles in top quark decay. There has been a good deal of recent interest in the search for one such new particle, for which the top quark decay provides by far the best discovery limit, i.e., the charged Higgs boson $H^{\pm}$ of the supersymmetric standard model [3].

There have been several exploratory works on $H^{\pm}$ search in the top quark decay at Tevatron and LHC energies [4–7]. They are based on one of the two distinctive properties of $H^{\pm}$ vis-à-vis the $W^{\pm}$ boson—(i) the preferential $H^{\pm}$ decay into the $\tau\nu$ channel relative to $e\nu$ or $\mu\nu$ [4,5], and (ii) the opposite states of τ polarization resulting from $H^{\pm}$ and $W^{\pm}$ decays [6,7]. In a recent work [8], we have suggested methods of sharpening up the $H^{\pm}$ signature in top quark decay by combining these two properties and applied them to $H^{\pm}$ search at Tevatron upgrade. Even with the best signature, however, the prospect of $H^{\pm}$ search at Tevatron upgrade was seen to be limited to a small part of the parameter space. In the present work, we shall analyze the prospect of $H^{\pm}$ search in top quark decay at LHC using these ideas. We shall see below that in this case one gets a viable signature over practically the full parameter space of $H^{\pm}$ coupling. Moreover, with a supplementary constraint on the accompanying hadronic jets, the signature remains viable over most of the kinematically allowed range of $H^{\pm}$ mass.

*Electronic address: dproy@theory.tifr.res.in

II. CHARGED HIGGS BOSON SIGNAL IN TOP QUARK DECAY

We shall concentrate on the charged Higgs boson of the minimal supersymmetric standard model (MSSM). Its couplings to fermions are given by

$$\mathscr{L} = \frac{g}{\sqrt{2}m_W} H^+ \{\cot\beta V_{ij} m_{u_i} \overline{u_i} d_{jL} + \tan\beta V_{ij} m_{d_j} \overline{u_i} d_{jR} + \tan\beta m_{\ell_j} \overline{\nu_j} \ell_{jR}\} + \text{H.c.}, \tag{2}$$

where V_{ij} are the Kobayashi-Maskawa (KM) matrix elements and $\tan\beta$ is the ratio of the vacuum expectation values of the two Higgs doublets. The QCD corrections are taken into account in the leading log approximation by substituting the quark mass parameters by their running masses evaluated at the $H^{\pm}$ mass scale [5]. Perturbative limits on the tbH Yukawa couplings of Eq. (2), along with the constraints from the low energy processes, such as $b \to s\gamma$ and B_d^0-$\overline{B_d^0}$ mixing, imply the limits [9]

$$0.4 < \tan\beta < 120. \tag{3}$$

In the most predictive form of the MSSM, characterized by a common supersymmetry-(SUSY-) breaking mass term at the grand unification point, one gets stronger limits [10]:

$$1 < \tan\beta < m_t/m_b. \tag{4}$$

Such a lower bound also follows from requiring the perturbative limit on the tbH Yukawa coupling to hold up to the unification point [11]. However, we shall consider the full range (3) of the phenomenologically allowed $\tan\beta$ parameter.

In the diagonal KM matrix approximation, one gets the decay widths

$$\Gamma_{t\to bW} = \frac{g^2}{64\pi m_W^2 m_t} \lambda^{1/2}\left(1, \frac{m_b^2}{m_t^2}, \frac{m_W^2}{m_t^2}\right)[m_W^2(m_t^2+m_b^2) + (m_t^2-m_b^2)^2 - 2m_W^4], \tag{5}$$

$$\Gamma_{t\to bH}=\frac{g^2}{64\pi m_W^2 m_t}\lambda^{1/2}\left(1,\frac{m_b^2}{m_t^2},\frac{m_H^2}{m_t^2}\right)[(m_t^2\cot^2\beta+m_b^2\tan^2\beta)\times(m_t^2+m_b^2-m_H^2)-4m_t^2m_b^2], \tag{6}$$

$$\Gamma_{H\to\tau\nu}=\frac{g^2 m_H}{32\pi m_W^2}m_\tau^2\tan^2\beta, \tag{7}$$

$$\Gamma_{H\to c\bar{s}}=\frac{3g^2 m_H}{32\pi m_W^2}(m_c^2\cot^2\beta+m_s^2\tan^2\beta). \tag{8}$$

From these, one can construct the relevant branching fractions

$$B_{t\to bH}=\Gamma_{t\to bH}/(\Gamma_{t\to bH}+\Gamma_{t\to bW}), \tag{9}$$

$$B_{H\to\tau\nu}=\Gamma_{H\to\tau\nu}/(\Gamma_{H\to\tau\nu}+\Gamma_{H\to c\bar{s}}). \tag{10}$$

It is the product of these two branching fractions that controls the size of the observable charged Higgs boson signal. The $t\to bH$ branching fraction has a pronounced dip at

$$\tan\beta=(m_t/m_b)^{1/2}\simeq 6, \tag{11}$$

where (6) has a minimum. Although this is partly compensated by a large value of the $H\to\tau\nu$ branching fraction, which is $\simeq 1$ for $\tan\beta>2$, the product still has a significant dip at (11). Consequently, the predicted charged Higgs boson signal will be very weak around this point as we shall see below.

The basic process of interest is $t\bar{t}$ pair production through gluon-gluon (or quark-antiquark) fusion followed by their decay into charged Higgs or W boson channels: i.e.,

$$gg\to t\bar{t}\to b\bar{b}(H^+H^-,H^\pm W^\mp,W^+W^-). \tag{12}$$

The τ decay of one or both the charged bosons leads to a single τ, $\tau\tau$, or $\ell\tau$ final state, where ℓ denotes e and μ. Each of these final states is accompanied by several hadronic jets and a large missing E_T (transverse energy) because of the neutrinos.

A brief discussion of the τ identification at hadron colliders is in order here. Starting with a missing-E_T trigger, the UA1, UA2, and CDF experiments have been able to identify τ as a narrow jet in its hadronic decay mode [12,13]. In particular, the CDF experiment has used the narrow jet cut to reduce the QCD jet background by an order of magnitude while retaining most of the hadronic τ events. Moreover, since the hadronic τ and QCD jet events dominantly populate the one-prong and multiprong channels, respectively, the prong distribution of the narrow jets can be used to distinguish the two. In particular, restricting to one-prong jets reduces the QCD background by another order of magnitude with very little loss to the hadronic τ signal. In this way, the CDF group [13] has been able to reduce the QCD background to a few tens of events in a data sample of integrated luminosity ~ 4 pb^{-1}, which could be subtracted out by extrapolation from higher prong channels. Consequently, they were able to identify the $W\to\tau\nu$ events and test W universality as well as put some modest constraints on top and $H^\pm$ masses from the level of the residual $\tau\nu$ events. In the present case, however, one would be looking for a few tens of hadronic τ events in a data sample of over 1000 times higher integrated luminosity and 10 times higher QCD jet cross section. So the QCD jet background cannot be controlled by the above method, even with b identification. Therefore, one cannot use the single τ channel for the charged Higgs boson search and even the $\tau\tau$ channel can be at best marginal. The best charged Higgs boson signature is provided by the $\ell\tau$ channel. The largest background comes from $W\to\ell\nu$, accompanied by QCD jets, which can be easily controlled by the above-mentioned jet angle and multiplicity cuts. Besides, the hard isolated lepton ℓ provides a more robust trigger than that by the missing E_T, particularly at the LHC. Therefore, we shall concentrate mainly on the $\ell\tau$ channel.

The $\ell\tau$ and $\tau\tau$ channels correspond to the leptonic decay of both the charged bosons in (12): i.e.,

$$\begin{array}{cccccccc} H^+ & H^-, & H^+ & W^-, & H^- & W^+, & W^+ & W^-, \\ \downarrow & \downarrow & \downarrow & \downarrow & \downarrow & \downarrow & \downarrow & \downarrow \\ \tau_L^+ & \tau_R^- & \tau_L^+ & \tau_L^-,l^- & \tau_R^- & \tau_R^+,l^+ & \tau_R^+,l^+ & \tau_L^-,l^- \end{array} \tag{13}$$

where L and R stand for left- and right-handed helicities of τ. By convention,

$$P_\tau\equiv P_{\tau^-}=-P_{\tau^+},\quad P_{\tau^\pm}=\frac{\sigma_{\tau_R^\pm}-\sigma_{\tau_L^\pm}}{\sigma_{\tau_R^\pm}+\sigma_{\tau_L^\pm}}. \tag{14}$$

For the $\ell\tau$ channel of our interest, the signal and the background come from the HW and WW terms, respectively. They correspond to exactly opposite states of τ polarization: i.e.,

$$P_\tau^H=+1,\quad P_\tau^W=-1. \tag{15}$$

Consequently, the use of the τ polarization effect for enhancing the signal to background ratio is particularly simple in this case as we shall see below. It may be noted here that the $\tau\tau$ channel has a better signal to background ratio because of the HH contribution as well as the enhancement of WH relative to WW by a combinatorial factor of 2 [5]. On the other hand, the polarization distinction is less simple. While both the τ's in the background have negative polarization, one or both of them have positive polarization in the signal. Nonetheless, the method of enhancing the signal to background ratio by the τ polarization effect discussed below can be extended to this channel, provided one can identify the $\tau\tau$ events from the QCD background.

III. τ POLARIZATION EFFECT

We shall concentrate on the one-prong hadronic decay channel of τ, which is best suited for τ identification. It accounts for 80% of hadronic τ decays and 50% of overall τ decays. The main contributors to the one-prong hadronic τ decay are [2]

$$\tau^\pm\to\pi^\pm\nu_\tau\ (12.5\%), \tag{16}$$

$$\tau^\pm\to\rho^\pm\nu_\tau\to\pi^\pm\pi^0\nu_\tau\ (24\%), \tag{17}$$

$$\tau^{\pm} \to a_1^{\pm} \nu \to \pi^{\pm}\pi^0\pi^0\nu_\tau \ (7.5\%), \tag{18}$$

where the branching fractions for the π and ρ channels include the small contributions from the K and $K^\star$ channels, respectively, since they have identical polarization effects. Note that only half of the a_1 decay channel contributes to the one-prong configuration. The masses and widths of ρ and a_1 are [2]

$$m_\rho(\Gamma_\rho) = 770(150) \ \text{MeV}, \quad m_{a_1}(\Gamma_{a_1}) = 1260(400) \ \text{MeV}. \tag{19}$$

One sees that the three decay processes (16), (17), (18) account for about 90% of the one-prong hadronic decay of τ. Thus, the inclusion of τ polarization effect in these processes will account for its effect in the inclusive one-prong hadronic decay channel to a good approximation.

The formalism relating τ polarization to the momentum distribution of its decay particles in (16), (17), (18) has been widely discussed in the literature [6–8,14,15]. We shall only discuss the main formulas relevant for our analysis. A more detailed account can be found in a recent paper by Bullock, Hagiwara, and Martin [7], which we shall closely follow. For τ decay into π or a vector meson (ρ, a_1), one has

$$\frac{1}{\Gamma_\pi}\frac{d\Gamma_\pi}{d\cos\theta} = \frac{1}{2}(1 + P_\tau \cos\theta), \tag{20}$$

$$\frac{1}{\Gamma_v}\frac{d\Gamma_{vL}}{d\cos\theta} = \frac{\frac{1}{2}m_\tau^2}{m_\tau^2 + 2m_v^2}(1 + P_\tau \cos\theta), \tag{21}$$

$$\frac{1}{\Gamma_v}\frac{d\Gamma_{vT}}{d\cos\theta} = \frac{m_v^2}{m_\tau^2 + 2m_v^2}(1 - P_\tau \cos\theta), \tag{22}$$

where v stands for the vector meson and L, T denote its longitudinal and transverse polarization states. The angle θ measures the direction of the meson in the τ rest frame relative to the τ line of flight, which defines its polarization axis. It is related to the fraction x of the τ energy momentum carried by the meson in the laboratory frame: i.e.,

$$\cos\theta = \frac{2x - 1 - m_{\pi,v}^2/m_\tau^2}{1 - m_{\pi,v}^2/m_\tau^2}. \tag{23}$$

Here, we have made the collinear approximation $m_\tau \ll p_\tau$, where all the decay products emerge along the τ line of flight in the laboratory frame.

The above distribution (20)–(22) can be simply understood in terms of angular momentum conservation. For $\tau^-_{R(L)} \to \nu_L \pi^-$, $v^-_{\lambda=0}$, it favors forward (backward) emission of π or longitudinal vector meson, while it is the other way around for transverse vector meson emission $\tau^-_{R(L)} \to \nu_L v^-_{\lambda=-1}$. Thus, the $\pi^\pm$s coming from $H^\pm$ and $W^\pm$ decays peak at $x=1$ and 0, respectively, and $\langle x_\pi \rangle_H = 2\langle x_\pi \rangle_W = 2/3$. Although the clear separation between the signal and the background peaks disappears after convolution with the τ momentum, the relative size of the average π momenta remains unaffected, i.e.,

$$\langle p_\pi^T \rangle_H \simeq 2\langle p_\pi^T \rangle_W \quad \text{for } m_H \simeq m_W. \tag{24}$$

Thus, the τ polarization effect (20) is reflected in a significantly harder $\pi^\pm$ momentum distribution for the charged Higgs boson signal compared to the W boson background. The same is true for the longitudinal vector mesons; but the presence of the transverse component dilutes the polarization effect in the vector meson momentum distribution by a factor [see Eqs. (21) and (22)]

$$\frac{m_\tau^2 - 2m_v^2}{m_\tau^2 + 2m_v^2}. \tag{25}$$

Consequently, the effect of τ polarization is reduced by a factor of $\sim 1/2$ in ρ momentum distribution and practically washed out in the case of a_1. Thus, the inclusive one-prong τ jet resulting from (16)–(18) is expected to be harder for the $H^\pm$ signal compared to the W boson background; but the presence of the transverse ρ and a_1 contributions makes the size of this difference rather modest. We shall see below that it is possible to suppress the transverse ρ and a_1 contributions and enhance the difference between the signal and the background in the one-prong hadronic τ channel even without identifying the individual mesonic contributions to this channel.

The key feature of vector meson decay, relevant for the above purpose, is the correlation between its state of polarization and the energy sharing among the decay pions. The transverse ρ and a_1 decays favor even sharing of energy among the decay pions, while the longitudinal ρ and a_1 decays favor asymmetric configurations where the charged pion carries either very little or most of the vector meson energy. It is easy to derive this quantitatively for the ρ decay. But a_1 decay is more involved. One can show from general considerations that the $a_{1T(L)} \to 3\pi$ decay favors the plane of the three pions in the a_1 rest frame being normal to (coincident with) the a_1 line of flight [15]. This agrees qualitatively with the above pattern of energy sharing. But one has to assume a dynamical model for a_1 decay to get a more quantitative result. We shall follow the model of Kuhn and Santamaria [16], based on the chiral limit (conserved axial-vector current approximation), which provides a good description of the $a_1 \to 3\pi$ data. One gets very similar pion energy distributions from the alternative model of Isgur *et al.* [17], as shown in [7]. A detailed account of the ρ and a_1 decay formalisms can be found in [7,8], along with the prescriptions for incorporating the finite ρ and a_1 widths. We shall only summarize the results below.

Figure 1 shows the ρ and a_1 decay distributions in the energy momentum fraction x', carried by the charged pion. The distributions are shown for both longitudinal and transverse polarization states of the vector mesons. The transverse ρ and a_1 distributions are clearly seen to vanish at the end points and peak in the middle, reflecting equipartition of energy momentum among the decay pions. In contrast, the longitudinal ρ distribution shows pronounced peaks near the end points $x'=0$ and 1, and the longitudinal a_1 at the former point. Note also that the direct pionic decay of τ (16) can be formally looked upon as a delta function contribution at $x'=1$ in this figure. Thus, one can suppress the unwanted ρ_T and a_{1T} contributions while retaining the π and at least good fractions of ρ_L and a_{1L} by restricting to the regions

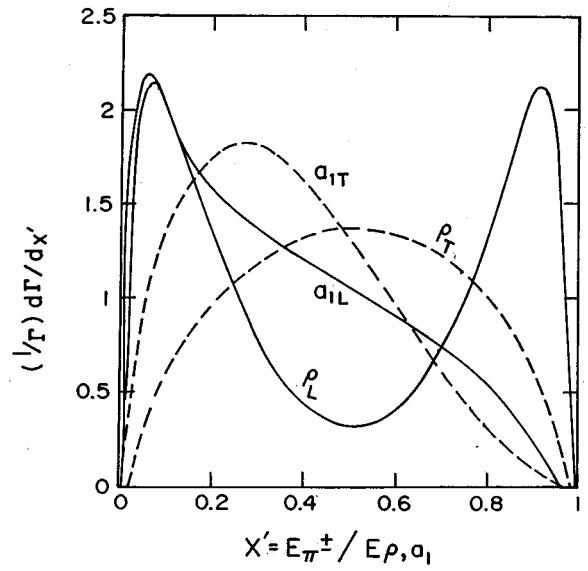

FIG. 1. Distributions of the $\rho^\pm \to \pi^\pm \pi^0$ and $a_1^\pm \to \pi^\pm \pi^0 \pi^0$ decay widths in the energy fraction carried by the charged pion, shown separately for the transverse and longitudinal states of ρ and a_1 polarization.

$x' \simeq 0$ and 1. We shall see below how this can be achieved even without identifying the individual mesonic contributions in τ decay.

IV. STRATEGY, RESULTS, AND DISCUSSION

As mentioned earlier, we are interested in the inclusive one-prong hadronic decay of τ, which is dominated by the $\pi^\pm$, $\rho^\pm$, and $a_1^\pm$ contributions (16), (17), (18). It results in a thin one-prong hadronic jet (τ jet) consisting of a charged pion along with 0, 1, or 2 π^0's, respectively. Since all the pions emerge in a collinear configuration, one can neither measure their invariant mass nor the number of π^0's. Thus it is not possible to identify the three mesonic states. But it is possible to measure the energy of the charged track and the accompanying neutral energy separately by measuring the momentum of the former in the tracking chamber and the total energy deposit in the electromagnetic and hadronic calorimeters surrounding it [18]. Thus, one has to devise a strategy to suppress the transverse vector meson contributions using these two pieces of information. We shall consider two such strategies below. In either case, a rapidity and a transverse energy cut of

$$|\eta| < 3 \quad \text{and} \quad E_T > 20 \ \text{GeV} \tag{26}$$

will be applied on the τ jet as well as the tagging lepton ℓ, where E_T includes the neutral contribution to the former [18]. We shall also apply isolation cuts to ensure that there is no hadronic jet within a cone of radius $\Delta R = (\Delta\eta^2 + \Delta\phi^2)^{1/2} = 0.4$ around the τ jet and the tagging lepton. It follows from (20)–(22) that, after the above E_T cut, the τ jet is dominated by the ρ_T and a_{1T} (ρ_L, a_{1L}, and π) contributions for the $W^\pm$ background ($H^\pm$ signal). Thus, the suppression of ρ_T and a_{1T} components leads to a better signal-to-background ratio besides enhancing the kinematic difference between the two.

The first strategy is to impose a calorimetric isolation cut on the τ jet, which requires the neutral E_T accompanying the charged track within a cone of $\Delta R = 0.2$ to be less than 5 GeV [19], i.e.,

$$E_T^{ac} \equiv E_T^0 < 5 \ \text{GeV}. \tag{27}$$

As we see from Fig. 1, this cut eliminates the ρ_T and a_{1T} contributions along with the $x' \simeq 0$ peaks of ρ_L and a_{1L}. It retains only the π and the $x' \simeq 1$ peak of the ρ_L contribution. This results in a substantially harder signal cross section relative to the background as well as a better signal-to-background ratio, but at the cost of a factor of ~ 2 drop in the signal size [20].

The second strategy is to plot the τ-jet events satisfying (26) as a function of

$$\Delta E_T = |E_T^{\rm ch} - E_T^0|, \tag{28}$$

i.e., the difference between the E_T of the charged track and the accompanying neutral E_T instead of their sum. It is clear from Fig. 1 that the even sharing of the transverse ρ and a_1 energies among the decay pions imply a significantly softer ΔE_T distribution for ρ_T and a_{1T} relative to ρ_L and a_{1L}. This results in a substantially harder signal cross section relative to the background when plotted against ΔE_T instead of E_T. Moreover, this is achieved at no cost to the signal size unlike the previous case.

In comparing the two methods, one notes that the first is easier to implement and, besides, it helps to suppress the level of QCD jet background as well. On the other hand, the second method has the advantage of a factor of ~ 2 larger cross section. While studying the $H^\pm$ signature at the Tevatron upgrade in [8], we had found the second method more viable in view of the limited size of the tt signal there. Since the size of this signal will be very large at the LHC, however, both the methods will be equally viable as we shall see below.

We have estimated $H^\pm$ signal and the $W^\pm$ background cross sections at the LHC energy of

$$\sqrt{s} = 14 \ \text{TeV}, \tag{29}$$

using a parton level Monte Carlo program with the recent structure functions of [21]. Instead of the differential cross section in E_T (or ΔE_T), we have plotted the corresponding integrated cross sections

$$\sigma(E_T) = \int_{E_T}^{\infty} \frac{d\sigma}{dE_T} dE_T \tag{30}$$

against the cutoff value of E_T (or ΔE_T). Figure 2 shows these cross sections for

$$\tan\beta = 3 \quad \text{and} \quad m_H = 120{,}140 \ \text{GeV} \tag{31}$$

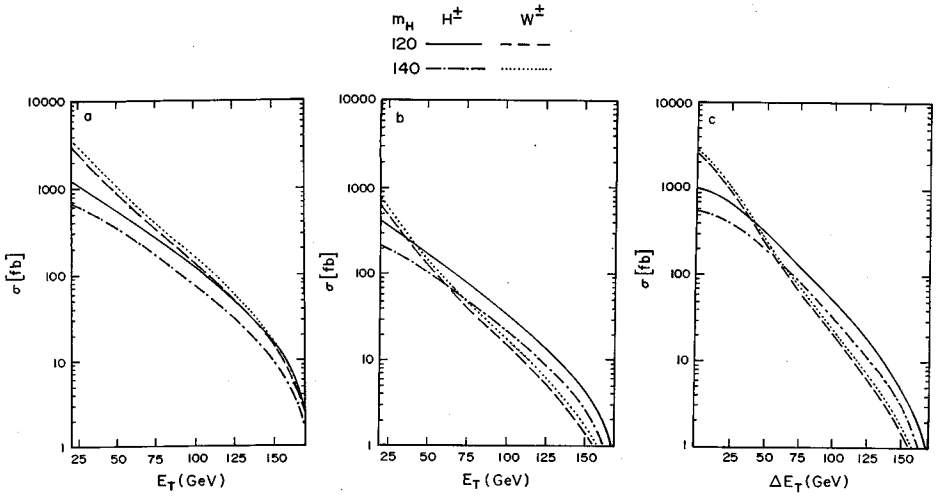

FIG. 2. The integrated one-prong hadronic τ-jet cross sections are plotted against cutoff values of the jet E_T in (a) without and (b) with the isolation cut. They are plotted against the cutoff-value of ΔE_T of the jet in (c). The $H^{\pm}$ signal ($W^{\pm}$ background) contributions are shown as solid (dashed) lines for $m_H = 120$ GeV and dot-dashed (dotted) lines for $m_H = 140$ GeV. We take $\sqrt{s} = 14$ TeV and $\tan\beta = 3$.

(a) for the raw signal, (b) using the calorimetric isolation cut (27), and (c) using ΔE_T instead of E_T.

There is a clear hardening of the signal curves relative to the background as one goes from Fig. 2(a) to 2(b) or 2(c). One could of course see a similar hardening in the corresponding differential cross sections. But the present plots are better suited to compare the relative merits of the three methods in extracting the signal from the background. For this purpose, the cutoff value of E_T (ΔE_T) is to be so chosen that one gets a viable signal to background ratio, i.e.,

$$H^{\pm} \text{ signal}/W^{\pm} \text{ background} \geq 1. \tag{32}$$

The resulting signal cross section, as given by the crossover point between the signal and background curves, is a reasonable criterion for the merit of the method. One clearly sees that this point is reached at a much larger value of the cutoff in Fig. 2(a), corresponding to a far greater sacrifice to the signal size, than in Fig. 2(b) or 2(c). The resulting signal cross sections for $m_H = 120$ and 140 GeV are ~ 20 fb and less than 1 fb in Fig. 2(a), going up to ~ 300 and 50 fb respectively, in Fig. 2(b) and about double these values in Fig. 2(c). It is remarkable that a simple calorimetric isolation cut (27) can enhance the signal-background separation so much and increase the effective signal cross section by over an order of magnitude. Of course, the signal cross section obtained via the ΔE_T distribution is still larger by a factor of ~ 2, as anticipated earlier.

To probe the $H^{\pm}$ discovery limits at LHC using the three methods, we have estimted the corresponding signal cross sections, satisfying (32), as functions of $\tan\beta$. These are shown in Figs. 3(a)–3(c) for a set of $H^{\pm}$ masses:

$$m_H = 80,100,120,140,150,160 \text{ GeV}. \tag{33}$$

There is a clear dip at $\tan\beta \simeq 6$ as anticipated in (11). One sees a gap in the $\tan\beta$ space around this region where the raw signal of Fig. 3(a) is clearly not viable. But the improved signals obtained via the calorimetric isolation cut [Fig. 3(b)] or the ΔE_T distribution [Fig. 3(c)] remain $\gtrsim 100(1)$ fb for

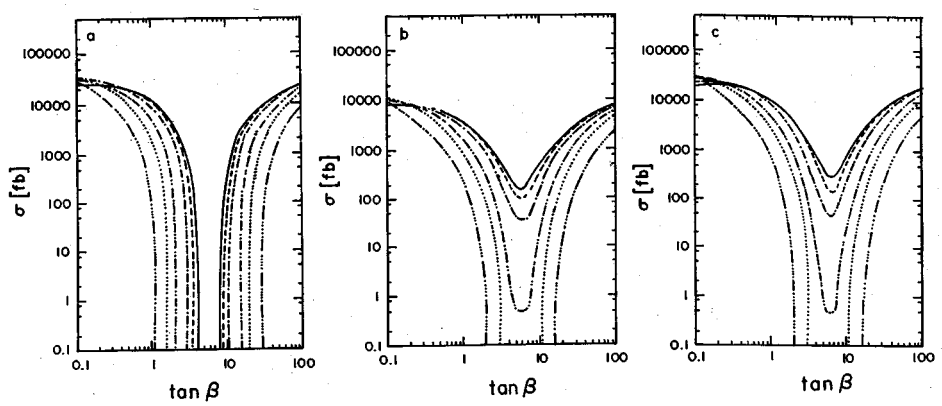

FIG. 3. The signal cross sections of Figs. 2(a)–2(c) satisfying a signal to background ratio ≥ 1 are shown as functions of $\tan\beta$ for $m_H = 80,100,120,140,150,160$ GeV by solid, dashed, dot-dashed, double dot-dashed, dotted, and multidot-dashed lines, respectively.

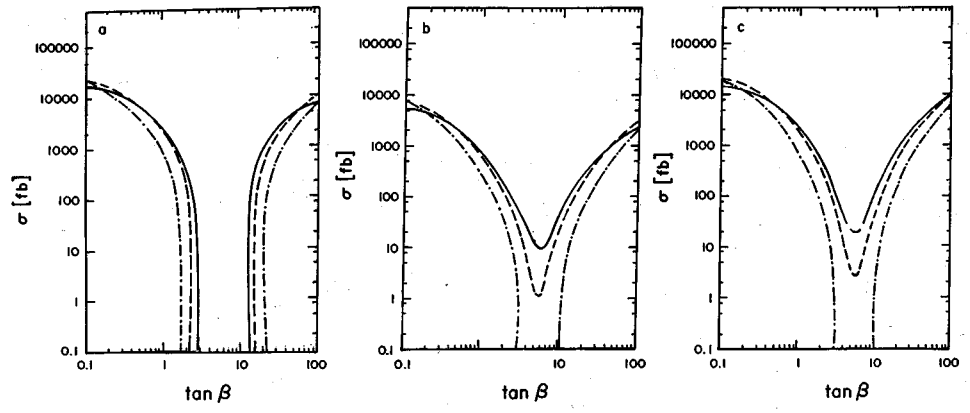

FIG. 4. The signal cross sections are shown as in Fig. 3, but with an additional cut of $E_T^{\rm jet}<30$ GeV on the second hardest accompanying jet, for $m_H=140,150,160$ GeV by solid, dashed and dot-dashed lines, respectively.

$m_H=120(140)$ GeV throughout the tanβ space. It may be noted here that one expects an integrated luminosity of

$$\int L dt \sim 100 \text{ fb}^{-1} \tag{34}$$

from the high luminosity run of the LHC. For a signal size of ~ 1 fb satisfying (32), it corresponds to $H^\pm$ signal and $W^\pm$ background events of ~ 100 each. Since the latter can be predicted from the number of tt events in the dilepton ($\ell^+\ell^-$) channel using W universality, this will correspond to a $\sim 10\sigma$ signal for the $H^\pm$ boson. Thus a signal size of ~ 1 fb in Fig. 3 will constitute a viable signal for the high luminosity run of LHC. This means that the improved signatures for $H^\pm$ boson search at LHC are viable up to $m_H=140$ GeV over the full tanβ space.

It may appear from Fig. 3 that for extreme values of tan$\beta(\lesssim 1$ or $\gtrsim 50)$, where the raw signal of Fig. 3(a) is already large, there is no advantage in going to Fig. 3(b) or 3(c). It should be noted, however, that in this case, the τ polarization effect can serve as an independent test for the $H^\pm$ signal. The hardening (softening) of the signal (background) cross section of Fig. 2 or, equivalently, the corresponding differential cross section [8], as one imposes the calorimetric isolation cut or goes to the ΔE_T variable, is a distinctive prediction of the τ polarization effect that holds independent of tanβ.

Finally, one can push the viability of these two signatures to still higher values of m_H with a suitable cut on the accompanying hadronic jets. For this purpose, one exploits the fact that for $m_H \simeq m_t$, the accompanying b jet in the $t\to bH(W)\to b\tau\nu$ decay is necessarily soft for the H signal but not for the W background [5]. Thus, the WW background can be suppressed without sacrificing the HW signal by imposing a kinematic cut of

$$E_T^{\rm jet}<30 \text{ GeV} \tag{35}$$

on all but one of the accompanying hadronic jets. Of course, in the process one would be sacrificing both the signal and background events which are accompanied by a hard QCD jet, which implies a reduction of the signal size without affecting the signal-to-background ratio. But we do not expect this reduction factor to be very large. Moreover, if there is a reasonable b identification efficiency at the LHC, then one can bypass this problem by imposing this cut on one of the identified b jets.

Figures 4(a)–4(c) shows the tanβ distribution of the signal cross sections satisfying (32), after this kinematic cut. The cross sections are shown only for the high values of m_H (140, 150, and 160 GeV), for which the cut is relevant. There is again a large gap in the tanβ space where the raw signal is not viable [Fig. 4(a)]. But the improved signals via the calorimetric isolation cut [Fig. 4(b)] or the ΔE_T distribution [Fig. 4(c)] remain $>10(1)$ fb for $m_H=140(150)$ GeV throughout the tanβ parameter space. Thus, they provide unambiguous signatures for $H^\pm$ boson search up to $m_H=140$ and 150 GeV at the low and high luminosity runs of LHC, corresponding to integrated luminosities of 10 and 100 fb^{-1}, respectively. In fact, for the high luminosity run, the signatures remain viable over the full tanβ space up to a $H^\pm$ mass of 155 GeV, i.e., within 20 GeV of the parent top quark mass.

In summary, we have explored the prospect of charged Higgs boson search in top quark decay at the LHC, taking advantage of the opposite states of τ polarization resulting from the $H^\pm$ and $W^\pm$ decays. We have concentrated on the most promising channel for $H^\pm$ search, i.e., the $\ell\tau$ channel, followed by the inclusive decay of τ into a one-prong hadronic jet. Two practical methods of sharpening up the $H^\pm$ signature, using the τ polarization effect, have been studied. The resulting signatures are shown to be viable over the full parameter space of tanβ up to $m_H=140$ GeV. Moreover, with a kinematic cut on the accompanying hadronic jets, one can stretch their viability up to $m_H=150$–155 GeV, i.e., within 20 GeV of the parent top quark mass.

ACKNOWLEDGMENTS

The work of S.R. was partially supported by a project (DO No. SR/SY/P-08/92) of the Department of Science and Technology, Government of India.

[1] CDF Collaboration, F. Abe *et al.*, Phys. Rev. Lett. **74**, 2626 (1995); D0 Collaboration, S. Abachi *et al.*, *ibid.* **74**, 2632 (1995).

[2] Particle Data Group, L. Montanet *et al.*, Phys. Rev. D **50**, 1173 (1994).

[3] J.F. Gunion, H.E. Haber, G. Kane, and S. Dawson, *The Higgs Hunters' Guide* (Addison-Wesley, Reading, MA, 1990).

[4] V. Barger and R.J.N. Phillips, Phys. Rev. D **41**, 884 (1990); A.C. Bawa, C.S. Kim, and A.D. Martin, Z. Phys. C **47**, 75 (1990); R.M. Godbole and D.P. Roy, Phys. Rev. D **43**, 3640 (1991).

[5] M. Drees and D.P. Roy, Phys. Lett. B **269**, 155 (1991); D.P. Roy, *ibid.* **283**, 403 (1992).

[6] R.M. Barnett *et al.*, in *Research Directions for the Decade*, Proceedings of the Summer Study on High Energy Physics, Snowmass, Colorado, 1990, edited by E.L. Berger (World Scientific, Singapore, 1991); B.K. Bullock, K. Hagiwara, and A.D. Martin, Phys. Rev. Lett. **67**, 3055 (1991); D.P. Roy, Phys. Lett. B **277**, 183 (1992).

[7] B.K. Bullock, K. Hagiwara, and A.D. Martin, Nucl. Phys. **B395**, 499 (1993).

[8] Sreerup Raychaudhuri and D.P. Roy, Phys. Rev. D **52**, 1556 (1995).

[9] V. Barger, J.L. Hewett, and R.J.N. Phillips, Phys. Rev. D **41**, 3421 (1990); J.F. Gunion and B. Grzadkowski, Phys. Lett. B **243**, 301 (1990); A.J. Buras *et al.*, Nucl. Phys. **B337**, 284 (1990).

[10] G. Ridolfi, G.G. Ross and F. Zwirner, in *Proceedings of the ECFA Large Hadron Collider Workshop*, Aachen, Germany, edited by G. Jarlskog and D. Rein (CERN Report No. 90-10, Geneva, Switzerland, 1990), Vol. II, p. 608.

[11] J. Bagger, S. Dimopoulos, and E. Masso, Phys. Rev. Lett. **55**, 920 (1985).

[12] UA2 Collaboration, J. Alitti *et al.*, Phys. Lett. B **280**, 137 (1992); UA1 Collaboration, C. Albajar *et al.*, *ibid.* **251**, 459 (1991).

[13] CDF Collaboration, F. Abe *et al.*, Phys. Rev. Lett. **72**, 1977 (1994).

[14] Y.S. Tsai, Phys. Rev. D **4**, 2821 (1971); P. Aurenche and R. Kinnunen, Z. Phys. C **28**, 261 (1985); K. Hagiwara, A.D. Martin, and D. Zeppenfeld, Phys. Lett. B **235**, 198 (1990).

[15] A. Rouge, Z. Phys. C **48**, 75 (1990).

[16] J.H. Kuhn and A. Santamaria, Z. Phys. C **48**, 445 (1990).

[17] N. Isgur, C. Morningstar, and C. Reader, Phys. Rev. D **39**, 1357 (1989).

[18] See, e.g., CMS Technical Report No. CERN/LHCC 94-38, 1994 (unpublished).

[19] Depending on the energy resolution of the calorimeters, this can be increased up to 10 GeV without affecting the results significantly. This observation is important, in particular, for the high luminosity run of LHC where the calorimetric energy resolution is likely to get degraded by the pileup.

[20] Such an isolation cut was considered in the context of SSC by R.M. Barnett, R. Cruz, J.F. Gunion, and B. Hubbard, Phys. Rev. D **47**, 1048 (1993). However, these authors considered only the pion contribution to the τ jet. It is clear from our Fig. 1, that the isolation cut would retain the $x' \simeq 1$ peak of the ρ_L, which is comparable to the pion contribution.

[21] A.D. Martin, R.G. Roberts, and W.J. Stirling, Phys. Lett. B **306**, 145 (1993); **309**, 492 (1993).